

DISSOLUTION OF A COPPER WIRE DURING A HOT-DIPPING PROCESS USING A SnCu1 LEAD-FREE SOLDER

RAZTAPLJANJE BAKRENE ŽICE MED VROČIM OMAKANJEM PRI UPORABI SPAJKE BREZ SVINCA SnCu1

Darja Steiner Petrovič¹, Jožef Medved², Grega Klančnik^{2,3}

¹Institute of Metals and Technology, Lepi pot 11, 1000 Ljubljana, Slovenia

²University of Ljubljana, Faculty of Natural Sciences and Engineering, Aškerčeva 12, 1000 Ljubljana, Slovenia

³Institute for Foundry and Heat Treatment, Litostrojska 60, 1000 Ljubljana, Slovenia
darja.steiner@imt.si

Prejem rokopisa – received: 2013-09-04; sprejem za objavo – accepted for publication: 2013-10-28

Thermodynamic arguments and calculations were used to describe a complete dissolution of a copper wire in a SnCu1 lead-free solder during hot-dipping at 400 °C. For the calculation of the phase diagram the newly reviewed Gibbs energies of the phases were used. The experimental investigation involved a visual inspection, stereomicroscopy, scanning electron microscopy (FE-SEM/EDX) and a thermal analysis (DSC). The results showed that the dissolution of the copper wire during hot dipping at a selected working temperature can be attributed to the increased solubility of the copper in the liquid solder and a prolonged time of dipping. Thus, the applied temperature was too high for the geometry, the volume-to-surface ratio, of the selected fuse element. Laboratory simulation tests performed at 303 °C showed a much slower kinetics for the Cu pick-up.

Keywords: lead-free solder, copper, dissolution, hot dipping, thermodynamics

Neželeno raztapljanje tanke bakrene žice v kopeli spajke SnCu1 pri temperaturi 400 °C smo opisali s termodinamičnimi argumenti in izračuni. Za izračun faznega diagrama smo uporabili na novo optimirane Gibbsove energije posameznih faz. Eksperimentalno delo je obsegalo vizualni pregled, stereomikroskopijo, vrstično elektronsko mikroskopijo (FE-SEM/EDX) in termično analizo (DSC). Rezultati so pokazali, da je raztapljanje bakrene žice med omakanjem na izbrani delovni temperaturi posledica povečane topnosti bakra v talini spajke in predolgega časa omakanja za dano geometrijo bakrene žice, predvsem velikega razmerja med površino in prostornino. Laboratorijski simulacijski preizkusi, izvedeni pri temperaturi 303 °C, so pokazali veliko počasnejšo kinetiko raztapljanja tanke bakrene žice.

Ključne besede: spajke brez svinca, baker, raztapljanje, omakanje, termodinamika

1 INTRODUCTION

Fuses consist of one or more metallic conductors, known as the fuse element, and usually have a cylindrical or flat strip form. The surrounding media are granular silica quartz (SiO₂) in high-breaking-capacity (HBC) fuses, and boric acid in expansion fuses. The element and the surroundings are housed in a body of an insulating material (ceramic, fibre, melamine, etc.). The fuse element's edges are usually soldered to, or in an electric contact with, the fuse end caps.¹

Another process used in the electronics industry for the coating of copper wires is hot dipping. The process is carried out by immersing a pre-treated (e.g., cleaned, etched) substrate in a bath of a molten solder metal, or an alloy, for a specific time.

In recent years a new generation of solders has been developed in order to replace Pb-Sn solders with lead-free solder alloys. Many of the proposed alloy systems are Sn-rich alloys. Thermodynamic properties play a crucial role in the development of the new solder materials.²⁻⁵ Although a thermodynamic assessment cannot cover the whole situation relating to kinetic problems, the driving forces and formation energies of intermetallic compounds, which are the most important

parameters in the growth kinetics, may be subjected to the thermodynamics of the system. A precise thermodynamic assessment of a Cu-Sn system was given by Shim et al.² New data is not only essential for a new alloy design but also very important for understanding the reactions between solder alloys and substrate materials.

The major factors affecting a solder selection are the melting point of an alloy, the wetting characteristics, the cost, the availability, the environmental friendliness, etc. Reliability-related properties include the electrical and thermal conductivities, the mechanical strength, the shear and tensile properties, the fatigue resistance, the corrosion and oxidation resistance, the coefficient of thermal expansion and the formation of intermetallic compounds.⁶

The three major chemical properties affecting the use and the long-term reliability of solders⁶ are as follows:

- the solubility of Cu in the solder,
- the resistance to corrosion,
- the oxidation behaviour.

In the literature a lot of data about the formation of intermetallic compounds (IMCs) is available. Investigations of interfacial interactions and the formation of

IMCs involving a solid substrate and liquid soldering alloys have mainly focused on simple geometries, holding the solder joint above the melting temperature of the solder alloy at a single interface and then maintaining the system under isothermal conditions.⁷⁻⁹

The aim of the present case study was to highlight the thermodynamic background of an undesirable dissolution of a fuse element (in this case a copper wire) at the temperature of interest, in the process of hot dipping using an Sn-Cu lead-free solder. For the calculation of a phase diagram, the reviewed Gibbs energies of phases were modelled using substitutional and stoichiometric models. The optimized parameters are presented in Appendix A.

In the investigation, a visual inspection, chemical analysis, stereomicroscopy, scanning electron microscopy (FE-SEM/EDS) and thermal analysis (DSC) were carried out. In addition, thermodynamic calculations using ThermoCalc were performed in order to determine the failure analysis. The copper dissolution was investigated by hot dipping the Cu wire into a SnCu1 soldering bath.

2 EXPERIMENTAL WORK

The specimens under investigation were a mass fraction 99.9 % Cu wire and a lead-free solder declared as SnCu1, both of which are used in industrial production processes for special-purpose fuses (**Table 1**).

The cross-sections of the materials under investigation were metallographically prepared by grinding and polishing. FE-SEM/EDX analyses were performed on these cross-sections using a JEOL JSM 6500-F electron microscope. An X-Ray fluorescence spectrometer (Thermo Scientific Niton) was used to determine the chemical composition of the solder alloy.

The thermal analysis was performed using differential scanning calorimetry (DSC) in an STA-449 C Jupiter, Netzsch instrument. The DSC experiments were conducted under the static atmosphere of argon of a volume fraction 99.999 % purity to minimize the surface oxidation. The empty corundum crucible was taken as a reference. The linear temperature program for the heating was as follows: 25 °C to 280 °C to 25 °C. The heating rate was taken to be 5 K/min to minimize the effects relating to the apparatus and hysteresis of the characteristic temperatures (emphasis was given to a determination of the liquidus temperature). There was no isothermal step at the maximum temperature in order to avoid a possible loss of elements. The liquidus temperature was estimated assuming that the peak temperature of the last thermal event during heating represents the liquidus temperature.¹⁰ The solidus temperature was taken as the onset of the melting during heating. The construction of the tangents for the solidus temperature was made on the DSC cooling curve with an extrapolation of the peak slope down to the baseline.

The copper dissolution was investigated by hot dipping the Cu-wire in a SnCu1 soldering bath. The tests were performed at 400 °C and 303 °C. For the temperature control a K-type thermocouple was used, protected with a corundum tube and immersed into the soldering bath. The dipping was done in air atmosphere as the common procedure of preparing the SnCu coatings.

2.1 Thermodynamic model

The thermodynamic calculations for the Cu-Sn binary system were performed with ThermoCalc Classic (TCC). Additionally, a computer simulation of the solidification of the selected solder alloy was performed with the Scheil-Gulliver model for simulating the solidification path, knowing that an equilibrium distribution of the elements is inhibited with the relatively high cooling rates after the hot-dipping process. The thermodynamic calculations were done using various models for describing the Gibbs energies of phases.

2.2 Substitutional model

The disordered solution phases and their Gibbs free energies, G_m^P , of fcc, liquid and bcc are described with the following equation:

$$G_m^P = X_{Cu} {}^0G_{Cu}^P + X_{Sn} {}^0G_{Sn}^P + RT(X_{Cu} \ln X_{Cu} + X_{Sn} \ln X_{Sn}) + {}^{ex}G_m^P$$

where ${}^{ex}G_m$, X_{Cu} , R and T represent the excess molar Gibbs energy, the molar fraction of Cu, the gas constant (8.314 J mol⁻¹ K⁻¹) and the temperature (K) represent the molar Gibbs energy of pure Cu in the P phase (liquid, fcc, bcc). The Gibbs energy of pure element Cu in the P phase is given relative to SER (the standard element reference of 298.15 K). The excess contribution is modelled as:

$${}^{ex}G_m^P = X_{Cu} X_{Sn} ({}^0L_{CuSn}^P + {}^1L_{CuSn}^P (X_{Cu} - X_{Sn}) + {}^2L_{CuSn}^P (X_{Cu} - X_{Sn})^2)$$

representing a deviation from the ideal solution.

2.3 Stoichiometric model

The stoichiometric phases (Cu₃Sn, Cu₄₁Sn₁₁, Cu₁₀Sn₃ and Cu₆Sn₅) were modelled using the following formulation of the Gibbs energy with reference to the enthalpies of pure Cu and Sn in phase Φ (298.15 K):

$$G_m^{Cu_p Sn_q}(T) - p {}^0H_{Cu}^\Phi - q {}^0H_{Sn}^\Phi = \Delta_f G_{Cu_p Sn_q}(T) + p \cdot GSERCU(T) + q \cdot GHSERSN(T)$$

where $\Delta_f G_{Cu_p Sn_q}(T)$ represents the standard Gibbs free energy. Normally, this is represented with the linear temperature dependence:

$$\Delta_f G_{Cu_p Sn_q}(T) = a + b \cdot T$$

where a and b represent the optimized parameters. GHSERCU and GHSERSN are the Gibbs free energies of pure elements, Cu and Sn, also relative to the stable state at 298.15 K. The two-sublattice model can be represented with $(\text{Cu})_p(\text{Sn})_q$. The p and q symbols represent the atomic ratio (the location of a phase). The D03 phase, with a larger solubility, was modelled with a two-sublattice model: $(\text{Cu},\text{Sn})_{0.75}(\text{Sn},\text{Cu})_{0.25}$. More details are given in².

3 RESULTS AND DISCUSSION

Copper wire is used in the production of fuses. It has a widespread use in electronic applications due to its superior thermal and electrical conductivities. In this case study a commercial copper coil with a diameter $d = \pm 0.15$ mm was investigated (**Figure 1**).

Problems occurred when, in the industrial process of hot dipping, the Pb-Sn solder was replaced with a Sn-Cu lead-free solder (**Figure 2**). After a few seconds in the solder bath, declared as SnCu1, heated to $T = 400$ °C, the copper wire was completely dissolved.

The DSC melting curve of the solder material was performed to determine its liquidus temperature, which gives very important information required for determining the optimum parameters of hot dipping. The DSC melting curve obtained at a heating rate of 5 K/min is presented in **Figure 3**. The T_{onset} of the major endothermic reaction was around 223.9 °C. The enthalpy of this endothermic reaction was 48.15 J/g.

From the DSC response during heating, it is clear that the chemical composition of the investigated Sn-Cu alloy is very close to the eutectic composition. For non-eutectic compositions the melting curve would show a splitting into two separate peaks due to the sample containing the Cu solid solution in Sn and the eutectic.¹¹

Additionally, the chemical composition of the solder material of the Sn-Cu alloy system was identified using

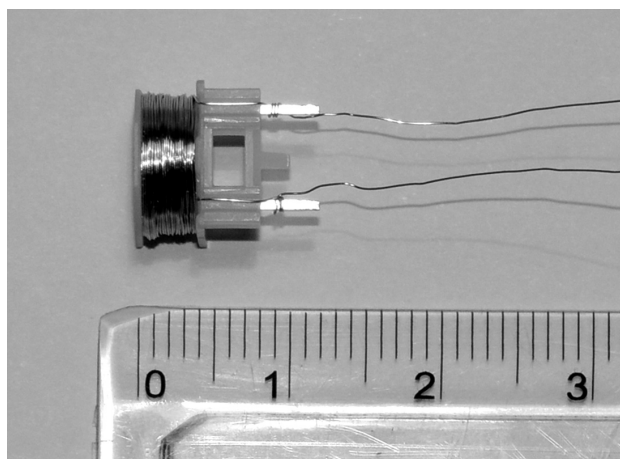


Figure 1: Fuse element (a Cu-coil)

Slika 1: Bakrena žica za varovalko

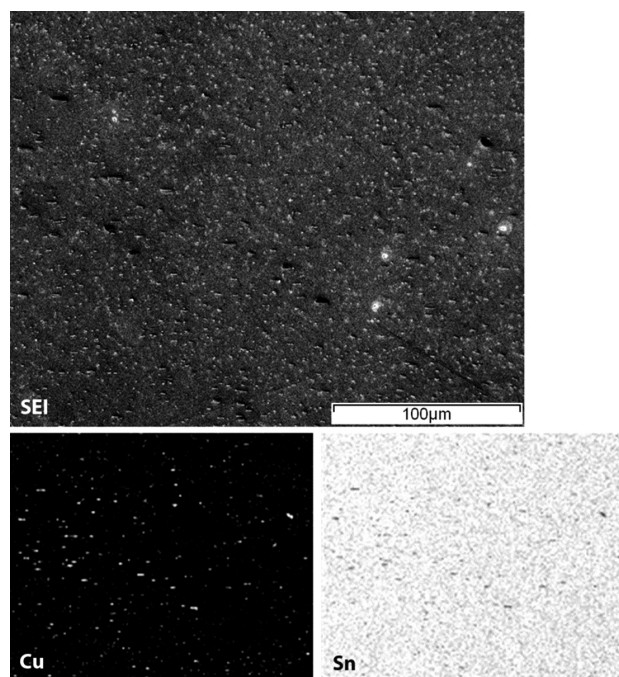


Figure 2: SE image and the corresponding X-ray elemental mapping showing the distribution of Cu and Sn in the solder

Slika 2: SEM-posnetek spajke in porazdelitev elementov Cu in Sn (EDX)

X-Ray fluorescence spectrometry. The chemical composition of the solder is given in **Table 1**.

Table 1: Chemical composition of the lead-free Sn-Cu solder in mass fractions ($w/\%$)

Tabela 1: Kemijska sestava spajke Sn-Cu v masnih deležih ($w/\%$)

	$w(\text{Sn})/\%$	$w(\text{Cu})/\%$
Solder Sn-Cu	99.183 ± 0.648	0.785 ± 0.034

The eutectic Sn-Cu solder alloy is one of the most popular lead-free alloys used for soldering in electronic applications.¹²

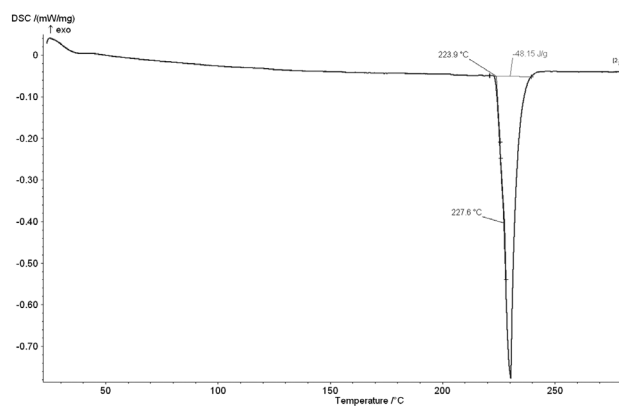


Figure 3: DSC heating curve for the solder material (the heating rate of 5 K/min)

Slika 3: DSC segrevalna krivulja za zlitino spajke (hitrost ogrevanja 5 K/min)

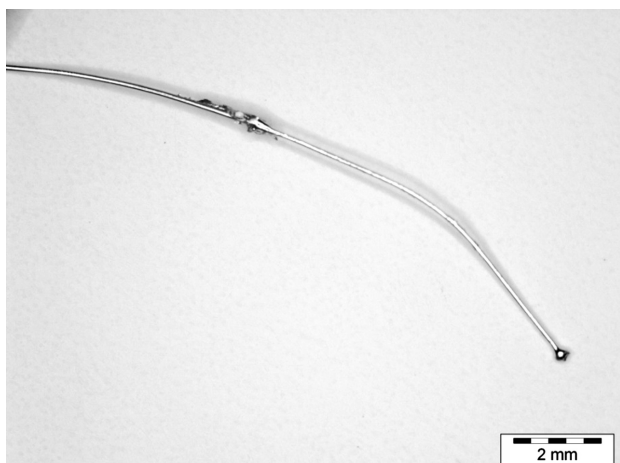


Figure 4: Cu wire after hot dipping in the SnCu1 bath at 303 °C for 10 s

Slika 4: Bakrena žica po omakanju pri temperaturi 303 °C, 10 s v kopeli SnCu1

Table 2: Average consumption of the Cu wire Δd during hot dipping at 303 °C in mass fractions

Tabela 2: Povprečno odtapljanje bakrene žice Δd med omakanjem pri 303 °C v masnih deležih

$T/^\circ\text{C}$	t/s	$\Delta d/\%$
303	10	30
303	20	60

The ability of a solder bath to pick up copper is directly related to the solubility of Cu in the major constituents.⁶ The dissolution kinetics of Cu in soldering reactions with Sn-Pb and Sn-Ag solders has already been described in^{13,14}.

In the present study the consumption of a Cu wire was investigated during the hot dipping of the wire into the soldering bath at 400 °C. At this temperature the soldering bath aggressively dissolves the whole of the Cu wire on contact. It has been reported that the suitable temperature to perform the soldering with the eutectic

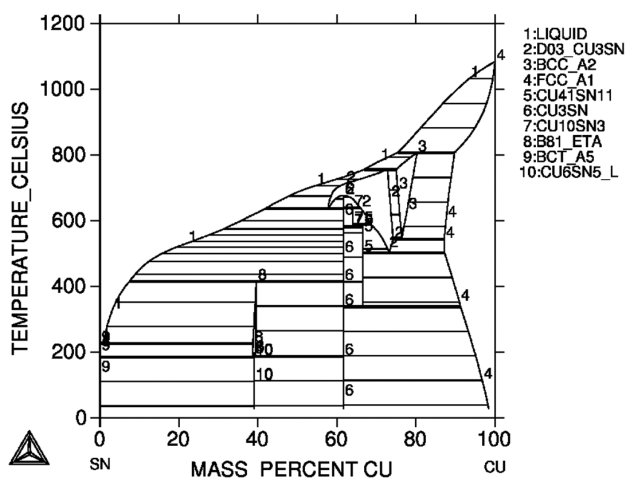


Figure 5: Binary phase diagram for Cu-Sn

Slika 5: Binarni fazni diagram Cu-Sn

Sn-0.7Cu alloy is 303 °C, because at this temperature the solder exhibits the lowest value of the surface tension.¹²

For this reason, comparison tests were also performed at 303 °C, showing much slower kinetics for the Cu pick-up. The results of the hot dipping at 303 °C are given in **Table 2**.

It was confirmed that a Cu wire with a diameter of approximately 140 μm to 153 μm is completely dissolved after a few seconds of being dipped in the solder bath at $T = 400$ °C. On the other hand, at $T = 303$ °C, the average Cu consumption measured after 10 s (**Figure 4**) and 20 s, as the difference between the initial diameter and that after hot dipping, was 30 % and 60 %, respectively.

The problem of the rapid dissolution of a Cu wire in a liquid solder can also be described using thermodynamic arguments. Using the CALPHAD method (CALculation of PHase Diagrams) the phase equilibria can be calculated with the relative Gibbs free energies of the phases present in a particular system.¹⁵ It is clear from the Cu-Sn phase diagram in **Figure 5** that the solid solubility of Cu in Sn at room temperature is practically zero. However, as the temperature increases, the solubility of Cu in Sn increases appreciably. The optimized parameters taken for the Cu-Sn system² are presented in Appendix A.

According to the Scheil-Gulliver model the liquidus temperature is 228 °C for Sn-0.7Cu (**Figure 6**). The calculated solidification process is in good agreement with the experimental one (**Figure 3**). With a decreasing temperature, the solidification of the liquid phase proceeds with the precipitation of Sn (the bct phase). Below 220 °C the precipitation of the fcc intermetallic takes place. The mass-fraction of all the stable phases in the Sn-0.7Cu system is presented in **Figure 7**.

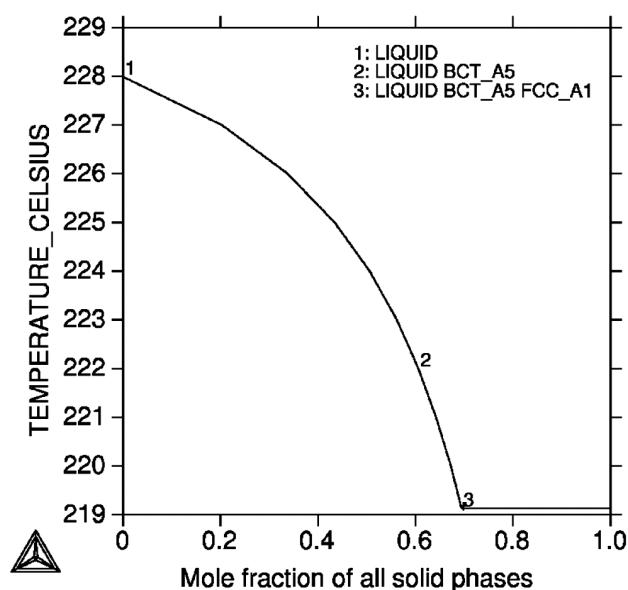


Figure 6: Solidification sequence of the Sn-0.7Cu alloy

Slika 6: Potek strjevanja zlitine Sn-0,7Cu

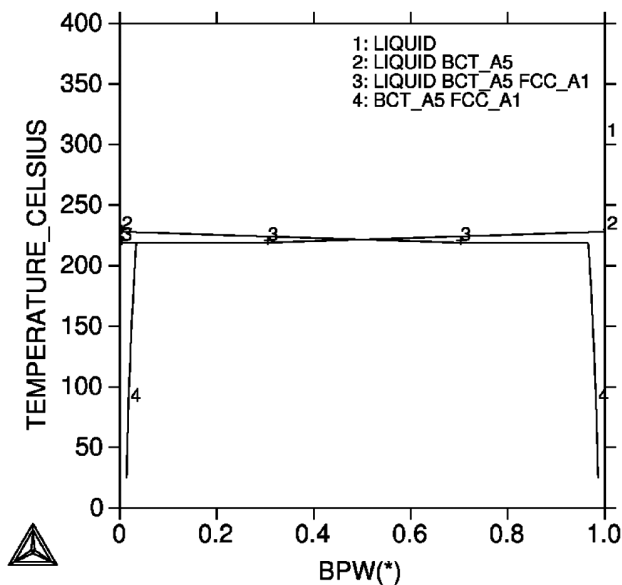


Figure 7: Mass fraction of stable phases in the Sn-0.7Cu system
Slika 7: Masni delež stabilnih faz v sistemu Sn-0,7Cu

During the soldering operation, materials from the solid substrate dissolve and mix with the solder, allowing a formation of intermetallic compounds (IMCs). It has been found that in Cu-Sn systems the formation of Cu_6Sn_5 is usually followed by Cu_3Sn .^{7,8} A compressive stress is generated as a result of the volume expansion during the growth of IMCs, especially Cu_6Sn_5 .^{16,17} The initial formation of Cu_6Sn_5 , followed by Cu_3Sn , can be attributed to a larger driving force for the precipitation of Cu_6Sn_5 during the early stages of the Cu/Sn reaction. Furthermore, the Cu/Sn interface is typically covered by a Cu_6Sn_5 layer within a few milliseconds. After a prolonged Cu_6Sn_5 layer growth, Cu_3Sn begins to appear at the Cu/ Cu_6Sn_5 interface.^{8,9}

The growth of IMCs as a result of the interactions between the eutectic Sn-0.7Cu solder and the Cu-based alloy was studied by Dariavach et al.¹⁸ A thick scallop layer of η - Cu_6Sn_5 and a thin layer of ε - Cu_3Sn were observed at the interface. The total thickness of IMCs and the grain size of the η -phase increased with the increasing soldering time.¹⁸ As the interfacial reaction occurs between the substrate and the molten solder, the liquid structure of the solder significantly affects the reaction and the formation of interfacial compounds.

4 CONCLUSIONS

The thermodynamic assessment of Shim et al.² was the basis for the thermodynamic description of a Sn-Cu system. The optimization was performed using ThermoCalc Classic (TCC). The optimized parameters of the phases of interest in the Sn-Cu system are listed in Appendix A. The thermodynamic data were used to describe a complete dissolution of a Cu wire in a SnCu1 lead-free solder during hot dipping at 400 °C.

The melting behaviour as well as the chemical analysis of the investigated solder declared as SnCu1 confirmed the chemical composition of Sn-Cu to be very close to the eutectic one. The measured liquidus temperature was approximately 228 °C.

According to the Sn-Cu binary phase diagram the solubility of copper in tin increases with the temperature.

A rapid dissolution of the copper wire during hot dipping at the working temperature $T = 400$ °C is attributed to the increased solubility of copper in a liquid solder. The applied temperature was too high for the geometry of the selected fuse element (0.15-mm thick copper wire).

The kinetics of the Cu dissolution in the Sn-Cu solder was much slower at 303 °C. The average copper consumption measured after 10 s and 20 s was approximately 30 % and 60 %, respectively.

Better results for hot dipping would be obtained by lowering the temperature of the solder bath so that the layer of intermetallic compounds (IMCs) would form on the interface between the solder bath and the copper fuse element. By lowering the working temperature for hot dipping, the solubility of copper in the solder would decrease and the nucleation of IMCs would be ensured.

Appendix A: Optimized parameters for the Sn-Cu phase diagram²

```
LIQUID
CONSTITUENTS: CU,SN
G(LIQUID,CU;0)-H298(FCC_A1,CU;0) =
  298.15<T< 1358.02:
+12964.736-9.511904*T-5.849E-21*T**7+GHSERCU
  1358.02<T< 3200.00: +13495.481-9.922344*T-3.642E+29*T**(-9)
+GHSERCU
G(LIQUID,SN;0)-H298(BCT_A5,SN;0) =
  100.00<T< 505.08: +7103.092-14.087767*T+1.47031E-18*T**7
+GHSERSN
  505.08<T< 3000.00: +6971.587-13.814382*T+1.2307E+25*T**(-9)
+GHSERSN
L(LIQUID,CU,SN;0) = -9002.8-5.8381*T
L(LIQUID,CU,SN;1) = -20100.4+3.6366*T
L(LIQUID,CU,SN;2) = -10528.4
BCC_A2
2 SUBLATTICES, SITES 1: 3
CONSTITUENTS: CU,SN : VA
G(BCC_A2,CU:VA;0)-H298(FCC_A1,CU;0) = +GCUBCC
G(BCC_A2,SN:VA;0)-H298(BCT_A5,SN;0) = +GSNBCC
L(BCC_A2,CU,SN:VA;0) = -44821.6+51.2164*T
L(BCC_A2,CU,SN:VA;1) = -6876.5-56.4271*T
BCT_A5
CONSTITUENTS: CU,SN
G(BCT_A5,CU;0)-H298(FCC_A1,CU;0) = +GCUBCT
G(BCT_A5,SN;0)-H298(BCT_A5,SN;0) = +GHSERSN
L(BCT_A5,CU,SN;0) = 21000
CU10SN3
2 SUBLATTICES, SITES .769: .231
CONSTITUENTS: CU : SN
G(CU10SN3,CU:SN;0)-0.769 H298(FCC_A1,CU;0)-0.231
H298(BCT_A5,SN;0) =
-6655-1.4483*T+.769*GHSERCU+.231*GHSERSN
CU3SN
```

2 SUBLATTICES, SITES .75: .25
 CONSTITUENTS: CU : SN
 $G(\text{CU3SN,CU:SN};0) - 0.75 \text{ H298}(\text{FCC_A1,CU};0) - 0.25 \text{ H298}(\text{BCT_A5,SN};0) =$
 $-8194.2 - 2043 * T + 7.75 * \text{GHSERCU} + 2.25 * \text{GHSERSN}$
 CU41SN11
 2 SUBLATTICES, SITES .788: .212
 CONSTITUENTS: CU : SN
 $G(\text{CU41SN11,CU:SN};0) - 0.788 \text{ H298}(\text{FCC_A1,CU};0) - 0.212 \text{ H298}(\text{BCT_A5,SN};0) =$
 $-6323.5 - 1.2808 * T + 7.788 * \text{GHSERCU} + 2.212 * \text{GHSERSN}$
 CU6SN5
 2 SUBLATTICES, SITES .545: .455
 CONSTITUENTS: CU : SN
 $G(\text{CU6SN5,CU:SN};0) - 0.545 \text{ H298}(\text{FCC_A1,CU};0) - 0.455 \text{ H298}(\text{BCT_A5,SN};0) =$
 $-6869.5 - 1.589 * T + 5.45 * \text{GHSERCU} + 4.45 * \text{GHSERSN}$
 CU6SN5_L
 2 SUBLATTICES, SITES .545: .455
 CONSTITUENTS: CU : SN
 $G(\text{CU6SN5_L,CU:SN};0) - 0.545 \text{ H298}(\text{FCC_A1,CU};0) - 0.455 \text{ H298}(\text{BCT_A5,SN};0) =$
 $-7129.7 + 4.059 * T + 5.45 * \text{GHSERCU} + 4.45 * \text{GHSERSN}$
 DO3
 2 SUBLATTICES, SITES .75: .25
 CONSTITUENTS: CU,SN : CU,SN
 $G(\text{DO3,CU:CU};0) - \text{H298}(\text{FCC_A1,CU};0) = +\text{GCUBCC}$
 $G(\text{DO3,SN:CU};0) - 0.25 \text{ H298}(\text{FCC_A1,CU};0) - 0.75 \text{ H298}(\text{BCT_A5,SN};0) =$
 $+116674.85 + 4.8166 * T + 7.75 * \text{GSNBCC} + 2.25 * \text{GCUBCC}$
 $G(\text{DO3,CU:SN};0) - 0.75 \text{ H298}(\text{FCC_A1,CU};0) - 0.25 \text{ H298}(\text{BCT_A5,SN};0) =$
 $-10029.85 + 0.0285 * T + 7.75 * \text{GCUBCC} + 2.25 * \text{GSNBCC}$
 $G(\text{DO3,SN:SN};0) - \text{H298}(\text{BCT_A5,SN};0) = +\text{GSNBCC}$
 $L(\text{DO3,CU:CU,SN};0) = -1857.8 - 2.5311 * T$
 $L(\text{DO3,CU:CU,SN};1) = -2.9894 * T$
 $L(\text{DO3,CU,SN:SN};0) = +45850 - 42.2191 * T$
 FCC_A1
 2 SUBLATTICES, SITES 1: 1
 CONSTITUENTS: CU,SN : VA
 $G(\text{FCC_A1,CU:VA};0) - \text{H298}(\text{FCC_A1,CU};0) = +\text{GHSERCU}$
 $G(\text{FCC_A1,SN:VA};0) - \text{H298}(\text{BCT_A5,SN};0) = +\text{GSNFCC}$
 $L(\text{FCC_A1,CU,SN:VA};0) = -11106.95 + 2.0791 * T$
 $L(\text{FCC_A1,CU,SN:VA};1) = -15718.02 + 5.92467 * T$

Acknowledgements

The authors would like to acknowledge ETI, d. d., Izlake, Slovenia, for the supply of the specimens. The work was also supported by the Slovenian Research Agency (Pr. No. P2-0050 and P2-0344).

5 REFERENCES

- C. S. Psomopoulos, C. G. Karagiannopoulos, Temperature distribution of fuse elements during the pre-arcing period, *Electric Power Sys Res*, 61 (2002), 161–167
- J. H. Shim, C. S. Oh, B. J. Lee, D. N. Lee, Thermodynamic assessment of the Cu-Sn system, *Z Metallkd*, 87 (1996), 205–212
- S. Amore, S. Delsante, N. Parodi, G. Borzone, Calorimetric Investigation of the Cu-Sn-Bi lead-free solder system, *J Therm Anal Calorim*, 92 (2008), 227–232
- W. Chen, J. Kong, W. J. Chen, Effect of rare earth Ce on the microstructure, physical properties and thermal stability of a new lead-free solder, *J Mining Metallurgy B*, 47 (2011), 11–21
- P. Fima, A. Gazda, Thermal analysis of selected Sn-Ag-Cu alloys, *J Therm Anal Calorim*, 112 (2013), 731–737
- M. Abteu, G. Selvaduray, Lead-free solders in microelectronics, *Material Sci Engin*, 27 (2000), 95–141
- M. S. Park, R. Arroyave, Early stages of intermetallic compound formation and growth during lead-free soldering, *Acta Mater*, 58 (2010), 4900–4910
- M. S. Park, R. Arroyave, Concurrent nucleation, formation and growth of two intermetallic compounds (Cu6Sn5 and Cu3Sn) during the early stages of lead-free soldering, *Acta Mater*, 60 (2012), 923–934
- M. S. Park, S. L. Gibbons, R. Arroyave, Phase-field simulations of intermetallic compound growth in Cu/Sn/Cu sandwich structure under transient liquid phase bonding conditions, *Acta Mater*, 60 (2012), 6278–6287
- W. J. Boettinger, U. R. Kattner, K. W. Moon, J. H. Perepezko, DTA and Heat-flux DSC Measurements of Alloy Melting and Freezing, Special publication 960-15, National Institute of Standards and Technology, Washington 2006, 1–90
- A. S. Pedersen, N. Pryds, S. Linderth, P. H. Larsen, J. Kjoller, The determination of dynamic and equilibrium solid/liquid transformation data for Sn-Pb using DSC, *J Therm Anal Calorim*, 64 (2001), 887–894
- P. K. N. Satyanarayan, Reactive wetting, evolution of interfacial and bulk IMCs and their effect on mechanical properties of eutectic Sn-Cu solder alloy, *Adv Colloid Interface Sci*, 166 (2011), 87–118
- H. K. Kim, K. N. Tu, Rate of consumption of Cu in soldering accompanied by ripening, *Appl Phys Lett*, 67 (1995), 2002–2004
- A. Sharif, Y. C. Chan, Dissolution kinetics of BGA Sn-Pb and Sn-Ag solders with Cu substrates during reflow, *Mater Sci Eng B*, 106 (2004), 126–131
- H. L. Lukas, S. G. Fries, B. Sundman, *Computational Thermodynamics, The Calphad Method*, Cambridge University Press, Cambridge 2007
- A. Skwarek, M. Pluska, J. Ratajczak, A. Czerwinski, K. Witek, D. Szwagierczak, Analysis of tin whisker growth on lead-free alloys with Ni presence under thermal shock stress, *Mater Sci Eng B*, 176 (2011), 352–357
- A. Skwarek, M. Pluska, A. Czerwinski, K. Witek, Influence of laminate type on tin whisker growth in tin-rich lead-free solder alloys, *Mat Sci Eng B*, 177 (2012), 1286–1291
- N. Dariavach, P. Callahan, J. Liang, R. Fournelle, Intermetallic growth kinetics for Sn-Ag, Sn-Cu, and Sn-Ag-Cu lead-free solders on Cu, Ni, and Fe-42Ni substrates, *J Electron Mater*, 35 (2006), 1581–1591